DNA-TR-86-98

OZONE FORMATION AND ION CHEMISTRY IN OXYGEN RADIOLYSIS

R. P. Turco
F. Gilmore
R&D Associates
P. O. Box 9695
Marina del Rey, CA 90295

25 March 1986

Technical Report

CONTRACT No. DNA 001-85-C-0022

Approved for public release;
distribution is unlimited.

THIS WORK WAS SPONSORED BY THE DEFENSE NUCLEAR AGENCY
UNDER RDT&E RMSS CODE B310085466 P99QMXDB00099 H2590D.

Prepared for
Director
DEFENSE NUCLEAR AGENCY
Washington, DC 20305-1000

Destroy this report when it is no longer needed. Do not return to sender.

PLEASE NOTIFY THE DEFENSE NUCLEAR AGENCY, ATTN: STTI, WASHINGTON, DC 20305-1000, IF YOUR ADDRESS IS INCORRECT, IF YOU WISH IT DELETED FROM THE DISTRIBUTION LIST, OR IF THE ADDRESSEE IS NO LONGER EMPLOYED BY YOUR ORGANIZATION.

DISTRIBUTION LIST UPDATE

This mailer is provided to enable DNA to maintain current distribution lists for reports. We would appreciate your providing the requested information.

☐ Add the individual listed to your distribution list.

☐ Delete the cited organization/individual.

☐ Change of address.

NAME: _____

ORGANIZATION: _____

OLD ADDRESS	CURRENT ADDRESS
_____	_____
_____	_____
_____	_____

TELEPHONE NUMBER: ( ) _____

SUBJECT AREA(s) OF INTEREST:

_____ _____

_____ _____

_____ _____

DNA OR OTHER GOVERNMENT CONTRACT NUMBER: _____

CERTIFICATION OF NEED-TO-KNOW BY GOVERNMENT SPONSOR (if other than DNA):

SPONSORING ORGANIZATION: _____

CONTRACTING OFFICER OR REPRESENTATIVE: _____

SIGNATURE: _____

Director
Defense Nuclear Agency
ATTN: STTI
Washington, DC 20305-1000

Director
Defense Nuclear Agency
ATTN: STTI
Washington, DC 20305-1000

REPORT DOCUMENTATION PAGE

1a. REPORT SECURITY CLASSIFICATION UNCLASSIFIED	1b. RESTRICTIVE MARKINGS
2a. SECURITY CLASSIFICATION AUTHORITY N/A since Unclassified	3. DISTRIBUTION/AVAILABILITY OF REPORT Approved for public release; distribution is unlimited
2b. DECLASSIFICATION/DOWNGRADING SCHEDULE N/A since Unclassified	
4. PERFORMING ORGANIZATION REPORT NUMBER(S) RDA-TR-135603-003	5. MONITORING ORGANIZATION REPORT NUMBER(S) DNA-TR-86-98
6a. NAME OF PERFORMING ORGANIZATION R & D Associates 6b. OFFICE SYMBOL (If applicable)	7a. NAME OF MONITORING ORGANIZATION Director Defense Nuclear Agency
6c. ADDRESS (City, State and ZIP Code) P.O. Box 9695 Marina del Rey, CA 90295	7b. ADDRESS (City, State and ZIP Code) Washington, DC 20305-1000
8a. NAME OF FUNDING/SPONSORING ORGANIZATION 8b. OFFICE SYMBOL (If applicable)	9. PROCUREMENT INSTRUMENT IDENTIFICATION NUMBER DNA 001-85-C-0022
8c. ADDRESS (City, State and ZIP Code)	10. SOURCE OF FUNDING NUMBERS PROGRAM ELEMENT NO. 62715H; PROJECT NO. P99QMXD; TASK NO. B; WORK UNIT ACCESSION NO. DH008670

11. TITLE (Include Security Classification)
OZONE FORMATION AND ION CHEMISTRY IN OXYGEN RADIOLYSIS

12. PERSONAL AUTHOR(S)
Turco, Richard; Gilmore, Forrest

13a. TYPE OF REPORT	13b. TIME COVERED	14. DATE OF REPORT (Year, Month, Day)	15. PAGE COUNT
Technical	FROM 850901 TO 860325	860325	62

16. SUPPLEMENTARY NOTATION
This work was sponsored by the Defense Nuclear Agency under RDT&E RMSS Code B310085466 P99QMXDB00099 H2590D.

17. COSATI CODES			18. SUBJECT TERMS (Continue on reverse if necessary and identify by block number)
FIELD	GROUP	SUB-GROUP	Oxygen Radiolysis; Ozone; Ion Chemistry; Electron Impact Ionization
4	1		
20	8		

19. ABSTRACT (Continue on reverse if necessary and identify by block number)

Detailed electron-impact and chemistry calculations have been carried out for situations corresponding to a number of published oxygen radiolysis experiments. The results fit the measured ozone production values within 25 percent, provided that the neutralization reaction of O_4^+ with O_2^- or O_4^- yields two oxygen atoms, while the neutralization of O_4^+ or O_5^+ by O_3^- yields no odd oxygen species (O or O_3) except for that already present in the ions.

In addition, to explain the steady-state ozone concentration attained by long-duration irradiation, the reaction $O_3^- + O_3 \rightarrow O_2^- + 2\,O_2$ is required, with a rate coefficient within a factor of two of 5×10^{-13} cm^3/s at room temperature and probably a temperature dependence of about exp (-1000/T).

20. DISTRIBUTION/AVAILABILITY OF ABSTRACT	21. ABSTRACT SECURITY CLASSIFICATION
☐ UNCLASSIFIED/UNLIMITED ☒ SAME AS RPT. ☐ DTIC USERS	UNCLASSIFIED

22a. NAME OF RESPONSIBLE INDIVIDUAL	22b. TELEPHONE (Include Area Code)	22c. OFFICE SYMBOL
Betty L. Fox	(202)325-7042	DNA/STTI

DD FORM 1473, 84 MAR — 83 APR edition may be used until exhausted. All other editions are obsolete.

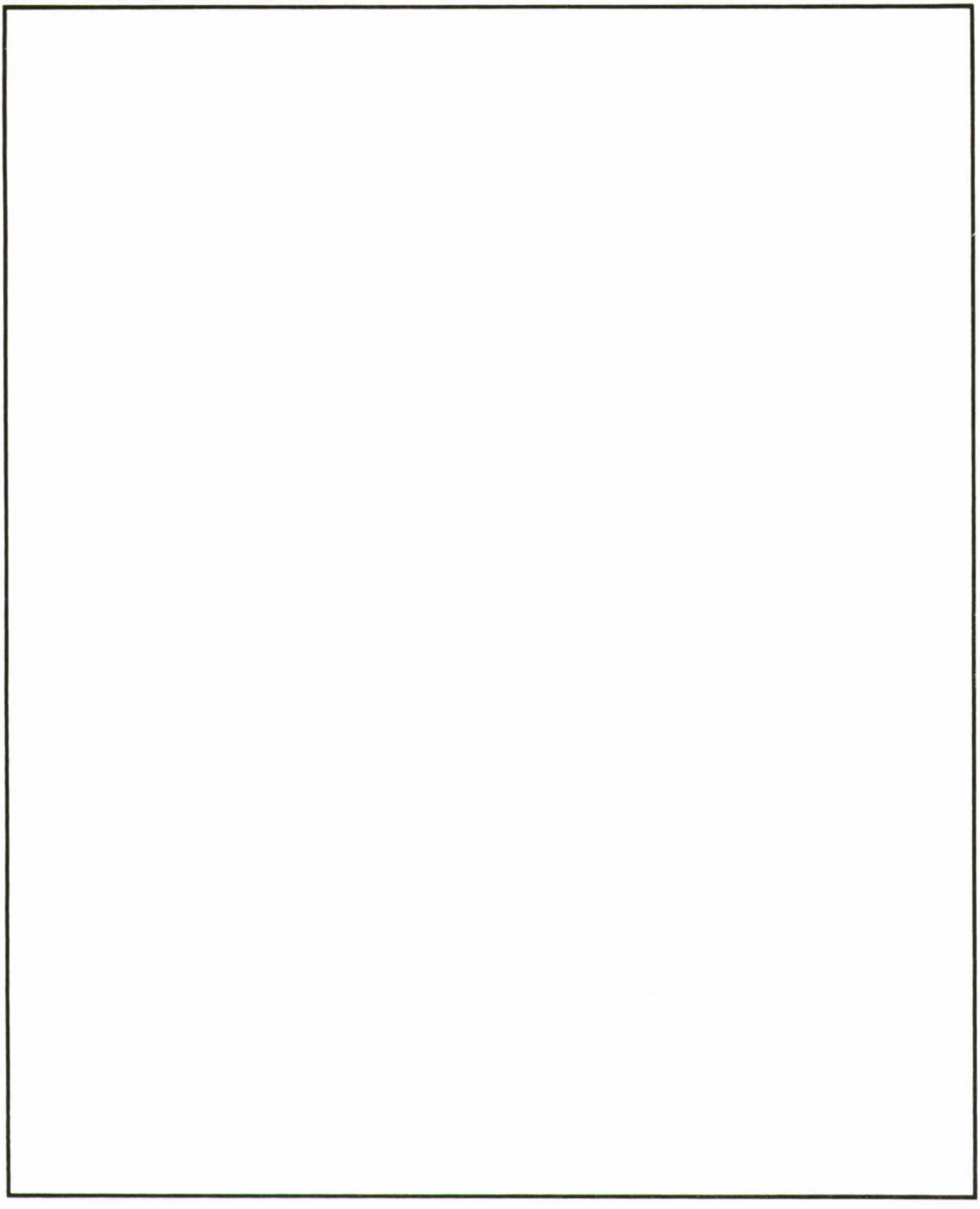

CONVERSION TABLE

Conversion factors for U.S. customary to metric (SI) units of measurement.

(Symbols of SI units given in parentheses)

To convert from	to	Multiply by
angstrom	meters (m)	1.000 000 X E -10
atmosphere (normal)	kilo pascal (kPa)	1.013 25 X E +2
bar	kilo pascal (kPa)	1.000 000 X E +2
barn	meter^2 (m^2)	1.000 000 X E -28
British thermal unit (thermochemical)	joule (J)	1.054 350 X E +3
calorie (thermochemical)	joule (J)	4.184 000
cal (thermochemical)/cm^2	mega joule/m^2 (MJ/m^2)	4.184 000 X E -2
curie	giga becquerel (GBq)*	3.700 000 X E +1
degree (angle)	radian (rad)	1.745 329 X E -2
degree Fahrenheit	degree kelvin (K)	$t_K = (t_{°F} + 459.67)/1.8$
electron volt	joule (J)	1.602 19 X E -19
erg	joule (J)	1.000 000 X E -7
erg/second	watt (W)	1.000 000 X E -7
foot	meter (m)	3.048 000 X E -1
foot-pound-force	joule (J)	1.355 818
gallon (U.S. liquid)	meter^3 (m^3)	3.785 412 X E -3
inch	meter (m)	2.540 000 X E -2
jerk	joule (J)	1.000 000 X E +9
joule/kilogram (J/kg)(radiation dose absorbed)	Gray (Gy)**	1.000 000
kilotons	terajoules	4.183
kip (1000 lbf)	newton (N)	4.448 222 X E +3
kip/inch^2 (ksi)	kilo pascal (kPa)	6.894 757 X E +3
ktap	newton-second/m^2 ($N-s/m^2$)	1.000 000 X E +2
micron	meter (m)	1.000 000 X E -6
mil	meter (m)	2.540 000 X E -5
mile (international)	meter (m)	1.609 344 X E +3
ounce	kilogram (kg)	2.834 952 X E -2
pound-force (lbf avoirdupois)	newton (N)	4.448 222
pound-force inch	newton-meter (N·m)	1.129 848 X E -1
pound-force/inch	newton/meter (N/m)	1.751 268 X E +2
pound-force/foot^2	kilo pascal (kPa)	4.788 026 X E -2
pound-force/inch^2 (psi)	kilo pascal (kPa)	6.894 757
pound-mass (lbm avoirdupois)	kilogram (kg)	4.535 924 X E -1
pound-mass-foot^2 (moment of inertia)	kilogram-meter^2 ($kg·m^2$)	4.214 011 X E -2
pound-mass/foot^3	kilogram/meter^3 (kg/m^3)	1.601 846 X E +1
rad (radiation dose absorbed)	Gray (Gy)**	1.000 000 X E -2
roentgen	coulomb/kilogram (C/kg)	2.579 760 X E -4
shake	second (s)	1.000 000 X E -8
slug	kilogram (kg)	1.459 390 X E +1
torr (mm Hg, 0° C)	kilo pascal (kPa)	1.333 22 X E -1

*THE BECQUEREL (BQ) IS THE SI UNIT OF RADIOACTIVITY; 1 BQ = 1 EVENT/S.

**THE GRAY (GY) IS THE SI UNIT OF ABSORBED RADIATION.

TABLE OF CONTENTS

TABLE OF CONTENTS (CONCLUDED)

LIST OF ILLUSTRATIONS

LIST OF TABLES

SECTION 1

INTRODUCTION

A high altitude nuclear explosion exposes the upper atmosphere to fast photoelectrons produced by absorption of the x-rays from the bomb, and to beta rays (megavolt electrons) from the radioactive debris. These electrons, and the secondary electrons they produce, directly dissociate some of the oxygen in the air, and also create ions and other reactive species that lead to further dissociation. The atomic oxygen thus created is of practical importance because it detaches electrons from negative ions, which increases the absorption of radio waves. In addition, it combines with molecular oxygen to form ozone (O_3), which is a strong infrared emitter, particularly in the 9 to 11 μm spectral region.

Current predictions of the amounts of atomic oxygen and ozone produced per unit energy deposited in the upper atmosphere are based on rather complex calculations of the relevant electron-impact and chemical processes, since no direct measurements are available. However, several laboratory measurements of the ozone production in irradiated air and oxygen at pressures typical of the lower atmosphere have been carried out and published. It is useful to utilize these experimental results to check or improve the complex air irradiation calculations, especially since the calculations involve several uncertain cross sections and rate constants. A logical procedure is to treat the pure oxygen case first, without the complication of nitrogen or water vapor reactions. This is done in the present analysis; even without the other air components it yields some significant results pertinent to atmospheric situations. A later report will treat the normal air case.

A few previous researchers have made limited comparisons of oxygen radiolysis measurements with chemical calculations. The most recent and most complete of these is that published by Willis et al. (Ref. 1) in 1970. Although these investigators were able to obtain reasonable agreement of calculations with measurements, they assumed rather than calculated the initial number of oxygen atoms produced by the irradiation. Moreover, although they used the best chemical rate coefficients available at that time, some of their values are now known to be inaccurate, and they neglected excited state reactions. Accordingly, a new and more complete analysis is needed in order to confirm or correct the conclusions of Ref. 1.

SECTION 2

INITIAL SPECIES PRODUCTION IN THE RADIOLYSIS OF OXYGEN

2.1 COMPUTATIONAL PROCEDURE.

The first step in making ozone calculations for comparison with the measurements is to determine the species produced initially by the electron bombardment. This requires a complex calculation of the excitation, dissociation and ionization processes that occur as the primary and secondary electrons slow down to thermal energies. Several groups of researchers have developed computer codes for making such calculations for any gas of interest, provided that the relevant electron-impact cross sections are input. Two groups have published a few results for pure oxygen (Refs. 2,3). However, neither group has given a set of results complete enough for the present purposes, nor did either employ the best available input cross sections.

Accordingly, new calculations of the initial species production in oxygen have been made at RDA. The results, are summarized in Table 1. The RDA calculations employed a "discrete energy bin" code, DPOSIT, which is based on a code originally developed by Dalgarno, Lejeune and Victor (see Ref. 4), modified by Stephens and Klein to handle higher energy primaries (Ref. 5), and further modified for greater input and output flexibility by the present writers and coworkers at RDA. It has been checked against a comparable code developed by Green and colleagues (Ref. 2) by applying it to irradiated air, and found to give results agreeing within 2 percent in every detail, when the same input cross sections are used.

Table 1. Initial production of atoms, ions and excited states in bombarded oxygen*.

Species	G Value (particles/100 eV)
$O_2(a^1\Delta_g)$	8.4†
$O_2(b^1\Sigma_g)$	1.7†
$O(^3P)$	4.0
$O(^1D)$	3.0
O_2^+	2.25
O^+	1.0
e	3.25

* The results are essentially identical for bombardment by 1 keV and 10 keV primary electrons.

† These values, which were used in the present chemistry calculations, were computed with 0.15% CO_2 in the O_2. In pure oxygen the values would be slightly larger, 8.9 and 1.8, respectively, but this makes a negligible difference in the ozone chemistry.

2.2 IMPORTANCE OF ELECTRON-IMPACT CROSS SECTIONS.

The principal source of error in electron degradation calculations is the inaccuracy in the basic electron-impact cross sections. Using limited measurements and theory, Porter, Jackman and Green (Ref. 6) derived algebraic expressions for the electronic excitation cross sections of oxygen, and Jackson, Garvey and Green (Ref. 7) did similarly for the ionization cross sections. However, more recent measurements, as well as some older measurements which they overlooked, show that their expressions are frequently significantly in error, sometimes by more than a factor of two. For the present analysis, a careful search for and evaluation of the best available cross sections was made, and the results were input to the DPOSIT code as numerical tables, avoiding the approximation of algebraic fits.

A complete DPOSIT calculation requires inputs and provides outputs for a large number of excited and ionized states. For present purposes, the most important outputs are the total amounts of oxygen atoms and O^+ and O_2^+ ions produced. In addition, the low metastable states of O_2 and O are involved in ozone-destroying reactions, and so should be included. Moreover, several other excited states also need to be included in the DPOSIT calculation, because excitation removes energy from the colliding electrons, leaving less energy for dissociation or ionization by subsequent collisions. In addition, dissociation of molecules by electron impact actually occurs by excitation of unstable electronic states which spontaneously dissociate; inclusion of such states is, of course, essential to the present analysis.

Since so much depends on input cross sections, the sources of the data used in the present calculations will be summarized below in some detail, starting with the lowest electronic states and working upward.

2.3 CROSS SECTIONS FOR NEUTRAL EXCITATION AND DISSOCIATION.

For the low O_2 metastable $a^1\Delta$ and $b^1\Sigma$ states, smooth curves were drawn through the data of Linder and Schmidt (Ref. 8), Trajmar et al. (Refs. 9 and 10), and Wakiya (Ref. 11), which are generally consistent in their overlapping energy regions. For the combined A, C and c states near 5 eV, which are too close together to be resolved in electron-impact measurements, the data of Refs. 10 and 11 were used. Since no measurements below 15 eV incident energy are available, the cross section was assumed to fall rapidly below this energy, in analogy to the rapid decrease of the cross section for the neighboring B state, discussed below.

A curve for the important $B^3\Sigma$ state, which contributes over half of the total oxygen atom production, was drawn through the data of Trajmar et al. (Ref. 10) and Wakija (Ref. 12). A similar curve for the low Rydberg states between 9.7 and 12.1 eV was based on the data of Wakiya (Ref. 12). For both states the published data extend only down to incident energies of 20 eV. Below this energy both cross sections were assumed to decrease rapidly, in accordance with a preliminary unpublished value by Shyn and Sharp (Ref. 13) for the B state at 15 eV.

As mentioned earlier, electron-impact dissociation of molecules generally takes place by excitation to unstable electronic states which spontaneously dissociate. In oxygen

this is believed to occur for essentially every excitation to the A + C + c and B states, and to every Rydberg state below 12.1 eV (the ionization energy of O_2). For the A + C + c and B states this conclusion follows from the Franck-Condon principle applied to the potential curves (Ref. 14) and also from the observed electron energy loss (Ref. 10-12) both of which indicate production of these states above their dissociation limits, so that the two oxygen atoms immediately fly apart. For the Rydberg states, the observed broadening of the ultraviolet absorption lines and the failure to detect corresponding emission lines indicate that these states "predissociate," i.e., spontaneously dissociate by interaction with neighboring dissociating states. The cross sections for all of these dissociating states could be combined into a single "dissociation cross section." However, because the energy lost by the incident electron varies with the particular state excited (the excess over the dissociation energy going into kinetic or excitation energy of the atomic fragments), it is desirable in DPOSIT calculations to treat each dissociating state separately.

In addition to the states discussed above, Porter et al. (Ref. 6) also considered a number of higher Rydberg states. Since none of these states are observed in optical emission, they must either predissociate or autoionize. Porter et al. arbitrarily assumed a 50-50 split between these two processes for most of the states, while photoabsorption and photoionization data (Ref. 15) show that autoionization is generally favored. In addition, the estimates of Porter et al. for the cross sections of these states were based on their estimates of the cross sections for the excited states of O_2^+

(the Rydberg "cores"), which they generally overestimated, as discussed below. Consequently, their Rydberg cross sections are probably too high.

It would be difficult to re-estimate cross sections for all of the 18 higher Rydberg states treated by Porter et al., and the results would still have considerable uncertainty. Fortunately, these states contribute less than 5 percent to the total dissociation cross section and less than 15 percent to the total ionization cross section. Moreover, the ionization error can be largely removed by constraining the total of all the ionization cross sections to the measured total ionization value. Accordingly, for the present DPOSIT calculations only the two lowest (and most strongly excited) Rydberg states above 12.1 eV, i.e., the $(a^4\Pi)3\ell$ and $(A^2\Pi)3\ell$ states at about 12.7 and 13.3 eV, were included. The cross sections used were those Porter et al. (Ref. 6). Although, as discussed above, these cross sections are probably too large, this is offset by the neglect of higher Rydberg states. In accordance with photoabsorption and photoionization data (Ref. 15), these states were assumed to dissociate spontaneously 30 percent of the time and autoionize 70 percent of the time.

2.4 CROSS SECTIONS FOR IONIZATION.

The cross section for ionizing O_2 to its ground ion state, $X\,^2\Pi$, was derived by subtracting the cross sections for Rydberg autoionization, just discussed, and for excited ion states, discussed below, from the total ionization cross section. The total cross section was taken from the measurements of Rapp and Englander-Golden (Ref. 16) up to 200 eV and of Schram et al. (Refs. 17, 18) above 500 eV, with a smooth

transition in the intermediate energy region where the data of the latter lie about 10 percent lower than those of the former.

Turner et al. (Ref. 19) measured the fraction of metastables in an O_2^+ beam produced by bombarding O_2 by electrons of energies up to 200 eV. This fraction rises from zero near 16 eV to a value of 0.33 above 70 eV. These results can be converted to a cross section for producing metastables by multiplying by the total oxygen ionization cross section, determined above, and by the fraction of the total ions ($O_2^+ + O^+$) that are O_2^+, measured by Rapp et al. (Ref. 20). The only known or predicted metastable state of O_2^+ is the $a^4\Pi$ state at 16.11 eV above the ground state of O_2 (Ref. 14). This O_2^+ state can be produced either directly or by the rapid radiative decay of the $b^4\Sigma$ and $c^4\Sigma$ states. However, the c-state apparently contributes little to the metastable production, since it primarily dissociates (Ref. 6). Accordingly, the a-state cross section has been obtained by subtracting from the metastable cross section, the cross section for producing the b-state, derived below. It might be noted that this new a-state cross section is about two-thirds of that employed by previous investigators (Refs. 2, 3, 5-7).

The cross sections for exciting a few emission bands of the O_2^+ $A^2\Pi$ state have been measured by Korol' et al. (Ref. 21), while a single point for one band at 100 eV has been given by McConkey and Woolsey (Ref. 22). However, the ratios of several band intensities given by Korol' et al. disagree seriously with the ratios obtained in radiative studies (Ref. 23). Moreover, the cross section of Korol' et al. falls off below 100 eV with unrealistic steepness. Fortunately, both this data and that of McConkey and Woolsey show that the A-state

cross section is less than one percent of the total ionization cross section, and so can be neglected for present purposes. (The correct cross section is clearly over an order of magnitude smaller than the semiempirical cross section derived in Ref. 7).

The cross section for exciting the O_2^+ $b^4\Sigma_g^-$ state has been measured with modern methods by five different groups of investigators (Refs. 22, 24-27), omitting the discordant measurements of Korol' et al. (Ref. 21) for reasons discussed earlier. All obtained curves of essentially the same shape, with a maximum around 100 eV, but their absolute magnitudes are significantly different, presumably due to differences in normalization (often a problem in this field). After correction for incomplete coverage of all the b-state emission bands, the cross sections of three of the investigating groups (Ref. 22, 24, 25) agree within 10 percent, while that of Borst and Zipf (Ref. 26) is about 40 percent lower, and that of Srivastava (Ref. 27) is about 50 percent lower.

As discussed earlier, the sum of the a- and b-state cross sections is fixed by the metastable measurements of Turner et al. (Ref. 19). If the b-state cross section of Refs. 22, 24 or 25 is assumed correct, the two cross sections are found to be roughly equal, while if that of Borst and Zipf (Ref. 26) or Srivastava (Ref. 27) is used, the b-state cross section is found to be about 1/2 or 1/3 that of the a-state.

Guidance in choosing among these alternatives can be obtained from optical measurements. Theory and measurements (Ref. 28) show that above a few hundred eV the electron-impact cross section for ionization is approximately proportional to the photoionization cross section (or differential optical

f-number) integrated over photon energies with a weighting factor that emphasizes the lower energies. Samson et al. (Ref. 29) have measured the partial photoionization cross sections for producing the b-state and the combined a + A states (unresolved), between threshold and 41 eV. Over most of this region the a + A cross section is about twice that of the b-state; moreover, it is quite large in the 16-18 eV region, which is below the threshold of the b-state. Since, as discussed above, optical emission data show that the contribution of the A state to the a + A combination is small, one concludes that the electron-impact cross section for producing the a-state is at least twice that for producing the b-state. This rules out the b-state cross sections of Refs. 22, 24 and 25. Of the two remaining sets of data, that of Borst and Zipf (Ref. 26) has been chosen, because they are more experienced workers and their data are smoother. (These values are only about half as large as the semiempirical values of Ref. 7.)

Electron impact on O_2 also produces several excited states of O_2^+ above the b-state. Apparently all of these states spontaneously dissociate into $O^+ + O$ (Ref 6), except for a small fraction of the c-state, which can be neglected for present purposes. Hence, they are included in the dissociative ionization cross section measured by Rapp et al. (Ref. 20). Much less is known about the partition of this cross section among the different excited states, but fortunately the DPOSIT calculations are less sensitive to the partition than to the total. Jackman et al. (Ref. 7) used the limited experimental evidence to divide these states into three groups, with thresholds at 20, 23 and 37 eV. Their groups and cross sections have been used in the present analysis, except that some adjustments were made to the 20 eV cross section to make

the total of the three agree with the measurements of Rapp et al. (Ref. 20).

2.5 RESULTS OF ELECTRON IMPACT CALCULATIONS.

The results of the DPOSIT calculation are summarized in table 1, with the following modifications: All predissociating excited states (discussed above) are replaced by their dissociation products, O + O or O^+ + O. The ground state (^3P) and metastable (^1D) atoms are tallied separately, which requires information about the electronic excitation of the dissociation products. The lowest dissociating states, A + C + c, and the dissociatively ionizing states below 20.7 eV, have insufficient energy to produce excited O atoms. The well-studied O_2 B state is known to dissociate into $O(^3P)$ + $O(^1D)$. The products of the higher excited states are less well established, but they contribute only about 20 percent of the total O atoms. Consequently, for these states the product assignments of Porter et al. (Ref. 6) have been used without further study. The small amount of $O(^1S)$ product they suggest is assumed here to be quenched immediately to $O(^3P)$.

The state of excitation of the ionized products, O_2^+ and O^+, has been ignored for present purposes, since on collision with O_2, excited O_2^+ is rapidly quenched and excited O^+ rapidly transfers its charge (Ref. 30). Such reactions might possibly yield metastable O_2 or O. but since there is no evidence for this possibility, it has been neglected. The DPOSIT calculation gives $G(O_2^+)$ = 2.42 and $G(O^+)$ = 1.04, where the G values are defined as the number of particles produced per 100 eV of deposited energy. The sum of these values, 3.46, slightly exceeds the experimental value, G(ions) = 3.25, derived from several careful measurements in oxygen showing that 30.8 eV is

required to produce each ion pair (Ref. 31). Although the difference is only 6 percent, the experimental value appears accurate to about 1 percent. Accordingly, for table 1 the calculated values of $G(O_2^+)$ and $G(O^+)$ have been decreased by 6 percent to give agreement with the ionization measurements.

The DPOSIT calculation was carried out for 1 keV primary electrons, while the oxygen radiolysis experiments generally used bombardment energies of hundreds of keV. However, theoretical calculations (Ref. 6) and ionization measurements (Refs. 31, 32) indicate that the G values are constant within about 5 percent for primary energies above 1 keV.

SECTION 3

CHEMICAL REACTIONS IN OXYGEN RADIOLYSIS

3.1 SOURCES OF BASIC DATA.

The chemical reactions believed to be involved in oxygen radiolysis are listed in table 2, together with their rate coefficients. Much of the chemical kinetic data is taken from standard compilations of laboratory measurements (Refs. 33-38), and some from more specialized papers (Ref. 39-49). Several rate coefficients, however, have not been measured, so have had to be estimated by analogy with similar reactions or by use of indirect evidence, as indicated in the footnotes to the table.

3.2 ION-MOLECULE PROCESSES.

In oxygen radiolysis, the initial bombardment produces O_2^+, O^+, and thermal electrons. The electrons very rapidly attach to O_2:

$$e + O_2 + O_2 \rightarrow O_2^- + O_2. \qquad (1)$$

The primary O^+ ions also rapidly charge exchange with O_2:

$$O^+ + O_2 \rightarrow O_2^+ + O. \qquad (2)$$

The O_2^- and O_2^+ ions then evolve by charge transfer, ion-neutral clustering, and other processes. The basic clustering reactions involve O_2:

$$O_2^- + O_2 + O_2 \rightarrow O_4^- + O_2 \qquad (3)$$

$$O_2^+ + O_2 + O_2 \rightarrow O_4^+ + O_2 \qquad (4)$$

Table 2. Reactions and Rate Coefficients for the Pure Oxygen System.

Reaction	Rate Coefficient[a]	Reference or Footnote
$e + O_2^+ \rightarrow O + O(^1D)$	$2.1 \times 10^{-7}(\frac{300}{T})^{0.63}$	33
$O^+ + O_2 \rightarrow O_2^+ + O$	1.9×10^{-11}	34
$O_2^+ + O_2 + O_2 \rightarrow O_4^+ + O_2$	$4.0 \times 10^{-30} (\frac{300}{T})^{2.93}$	39
$O_4^+ + O_2 \rightarrow O_2^+ + 2O_2$	$1.3 \times 10^{-4} (\frac{300}{T})^{2.93} e^{-6000/T}$	b
$e + O_4^+ \rightarrow O + O + O_2$	$2.0 \times 10^{-6} (\frac{300}{T})$	33
$O_4^+ + O \rightarrow O_2^+ + O_3$	3.0×10^{-10}	34
$O_2^+ + O_3 + O_2 \rightarrow O_5^+ + O_2$	$1.0 \times 10^{-28} (\frac{300}{T})^3$	c
$O_5^+ + O_2 \rightarrow O_2^+ + O_3 + O_2$	$3.3 \times 10^{-4} (\frac{300}{T})^3 e^{-7850/T}$	d
$e + O_5^+ \rightarrow O + 2O_2$	$2.0 \times 10^{-6} (\frac{300}{T})$	e
$O_4^+ + O_3 \rightarrow O_5^+ + O_2$	1.0×10^{-10}	f
$O_5^+ + O_2 \rightarrow O_4^+ + O_3$	$1.0 \times 10^{-11} e^{-1850/T}$	f
$e + O_2 + O_2 \rightarrow O_2^- + O_2$	$1.4 \times 10^{-29} (\frac{300}{T}) e^{-600/T}$	33
$O_2^- + O \rightarrow e + O_3$	1.5×10^{-10}	33
$O_2^- + O \rightarrow O^- + O_2$	1.5×10^{-10}	33
$O_2^- + O_2 (^1\Delta_g) \rightarrow e + 2O_2$	2.0×10^{-10}	34

Table 2. Reactions and Rate Coefficients for the Pure Oxygen System (Continued).

Reaction	Rate Coefficient	Reference or Footnote
$O^- + O \rightarrow e + O_2$	2.0×10^{-10}	33
$O^- + O_2 (^1\Delta_g) \rightarrow e + O_3$	3.0×10^{-10}	34
$O_2^- + O_3 \rightarrow O_3^- + O_2$	4.0×10^{-10}	33
$O_3^- + O \rightarrow O_2^- + O_2$	2.5×10^{-10}	34
$O_3^- + O_3 \rightarrow O_2^- + 2O_2$	$3.0 \times 10^{-11} e^{-1000/T}$	g
$O_2^- + O_2 + O_2 \rightarrow O_4^- + O_2$	$3.5 \times 10^{-31} (\frac{300}{T})$	33
$O_4^- + O \rightarrow O_3^- + O_2$	4.0×10^{-10}	34
$O_4^- + O_3 \rightarrow O_3^- + 2O_2$	3.0×10^{-10}	33
$O^+ + O_2^- \rightarrow O + O_2$	2.0×10^{-6}	h
$O^+ + O_4^- \rightarrow O + 2O_2$	2.0×10^{-6}	h
$O_2^+ + O^- \rightarrow O + O_2$	2.0×10^{-6}	h,i
$O_2^+ + O_2^- \rightarrow O + O + O_2$	2.0×10^{-6}	h
$O_2^+ + O_3^- \rightarrow O_2 + O_3$	2.0×10^{-6}	h
$O_2^+ + O_4^- \rightarrow O + O + 2O_2$	2.0×10^{-6}	h
$O_4^+ + O^- \rightarrow O + 2O_2$	2.0×10^{-6}	h

Table 2. Reactions and Rate Coefficients for the Pure Oxygen System (Concluded).

Reaction	Rate Coefficient	Reference or Footnote
$O_4^+ + O_2^- \rightarrow O + O + 2O_2$	2.0×10^{-6}	h
$O_4^+ + O_3^- \rightarrow O_3 + 2O_2$	2.0×10^{-6}	h
$O_4^+ + O_4^- \rightarrow O + O + 3O_2$	2.0×10^{-6}	h
$O_5^+ + O_2^- \rightarrow O_3 + 2O_2$	2.0×10^{-6}	h
$O_5^+ + O_3^- \rightarrow 2O_3 + O_2$	2.0×10^{-6}	h
$O_5^+ + O_4^- \rightarrow O_3 + 3O_2$	2.0×10^{-6}	h
$O + O_2 + O_2 \rightarrow O_3 + O_2$	$6.9 \times 10^{-34} \left(\frac{300}{T}\right)^{1.25}$	35
$O + O_3 \rightarrow O_2 + O_2$	$8.0 \times 10^{-12} e^{-2060/T}$	36
$O + O + O_2 \rightarrow O_2 + O_2$	$4.8 \times 10^{-33} \left(\frac{300}{T}\right)^{2}$	j
$O\ (^1D) + O_2 \rightarrow O + O_2\ (^1\Sigma_g^+)$	$2.6 \times 10^{-11} e^{67/T}$	36
$O\ (^1D) + O_2 \rightarrow O + O_2$	$6.0 \times 10^{-12} e^{67/T}$	37
$O\ (^1D) + O_3 \rightarrow O_2 + O_2$	1.2×10^{-10}	36
$O\ (^1D) + O_3 \rightarrow O + O + O_2$	1.2×10^{-10}	36
$O_2\ (^1\Delta_g) + O_2 \rightarrow O_2 + O_2$	$2.2 \times 10^{-18} \left(\frac{T}{300}\right)^{0.8}$	38
$O_2\ (^1\Sigma_g^+) + O_2 \rightarrow O_2\ (^1\Delta_g) + O_2$	3.8×10^{-17}	47,48
$O_2\ (^1\Delta_g) + O_3 \rightarrow O + 2O_2$	$1.2 \times 10^{-11} e^{-2400/T}$	38
$O_2\ (^1\Sigma_g^+) + O_3 \rightarrow O + 2O_2$	2.4×10^{-11}	49

Footnotes to Table 2

a. Rate constant units for bimolecular reactions are cm^3/sec, and for termolecular reactions, cm^6/sec.

b. The reverse rate coefficient is calculated using the forward rate coefficient and the equilibrium constant data of Payzant et al. (Ref. 40) and Conway and Janik (Ref. 41), $K_{eq} = 3.0 \times 10^{-26} e^{6000/T} cm^3$.

c. The value for He as the third body is about 1×10^{-28} cm^6/sec at 200 K (Ref. 34). The same value is used for O_2 as the third body at 300 K. Further, a temperature dependence of $(300/T)^3$ is assumed, as in the $O_2^+ + O_2 + O_2$ reaction (Ref. 39).

d. Calculated from the reverse rate coefficient and the equilibrium constant derived from the equilibria for $O_2^+ + O_2 + O_2 \rightleftharpoons O_4^+ + O_2$ and $O_4^+ + O_3 \rightleftharpoons O_5^+ + O_2$ (see footnotes b and f).

e. Assumed to have the same value as for $e + O_4^+$.

f. The forward reaction is estimated from other fast ion-neutral switching reactions (Ref. 34); the reverse reaction is calculated from the equilibrium constant of Dotan et al. (Ref. 42), $K_{eq} = 10\ e^{1850/T}$.

g. This rate coefficient was selected to have a room temperature value of about 10^{-12} cm^3/sec, as deduced in oxygen radiolysis experiments (Ref. 43), and an activation energy of about 2 kcal/mole, as deduced from temperature-dependent studies (Ref. 44). The present analysis suggests that this value may be an upper limit, and a more likely value is about half as large (see section 4.4).

h. Estimated high pressure value from References 45 and 46.

i. It is possible that the products are O + O + O, but this reaction appears to be unimportant both in radiolysis experiments and in the ambient or disturbed atmospheres.

j. The rate coefficient listed corresponds to N_2 as the third body (Refs. 33 and 38). Insufficient data are available at temperatures below 500 K with O_2 as the collision partner.

The importance of the clusters is principally in their greater thermochemical stability, which might prevent them from breaking up to yield oxygen atoms when they recombine with oppositely-charged ions (see next section). Ion molecule interchange reactions can also lead to ions of greater stability:

$$O_4^+ + O_3 \rightarrow O_5^+ + O_2. \qquad (5)$$

Such reactions have not been considered in past radiolysis studies.

In the case of negative ions, molecules with large electron affinities can scavenge negative charge by charge transfer. Two such reactions that are important in oxygen radiolysis are

$$O_2^- + O_3 \rightarrow O_3^- + O_2, \qquad (6)$$

and

$$O_4^- + O_3 \rightarrow O_3^- + O_2 + O_2. \qquad (7)$$

Previous radiolysis analyses have omitted the latter reaction.

Certain reactions can detach electrons or reduce complex ions to simpler ones, for example:

$$O_2^- + O \rightarrow e + O_3, \qquad (8)$$

$$O_3^- + O \rightarrow O_2^- + O_2, \qquad (9)$$

$$O_4^- + O \rightarrow O_3^- + O_2. \qquad (10)$$

However, at the high pressures typical of radiolysis experiments, such recycling reactions are overwhelmed by clustering reactions.

At pressures near one atmosphere, larger cluster ions such as O_6^+ and O_6^- are known to form, but few of their reaction rate coefficients are known. Equilibrium data (Ref. 41) indicate that their concentrations are small except below 200°K, so they have not been included in the present analysis.

3.3 ION-ION RECOMBINATION.

In radiolysis experiments, the charge produced by irradiation is neutralized primarily by recombination of positive with negative ions. In the present case, the positive ions are predominantly O_2^+ and O_4^+, and the recombination products can be O_2 or, if enough energy is available for dissociation, O + O. The distinction is important because the O atoms generated by ion-ion recombination can eventually form ozone and increase the ozone yield. If all recombination occurs via stable ions without dissociation, no net ozone production from ions results.

In the most recently published discussion of the ozone yield under various conditions of oxygen radiolysis (Ref. 1), it was suggested that reactions of the following sort lead to O-atom generation:

$$\left(O_2^+ \text{ or } O_4^+\right) + \left(O_2^- \text{ or } O_4^-\right) \rightarrow O + O + n\ O_2, \qquad (11)$$

while the following reactions do not:

$$\left(O_2^+ \text{ or } O_4^+\right) + O_3^- \rightarrow O_3 + n\ O_2. \qquad (12)$$

These suggestions have been adopted in the present calculations. We also assume that the recombination of O_5^+ with negative ions leads to $O_2 + O_3$ without O-atom production.

Measurements of ion-ion recombination at atmospheric pressure suggest a typical recombination coefficient of about 2×10^{-6} cm^3/sec (Refs. 45, 46). A specific study has been made by Wood et al. (Ref. 50) of ion-ion recombination rates in oxygen subject to low level continuous gamma irradiation. At pressures of 100-300 torr, an average coefficient of about 1.1×10^{-6} cm^3/sec was measured. At a pressure around 30 torr the coefficient decreased to about 0.9×10^{-6} cm^3/sec. Since most radiolysis experiments have been conducted at pressures near one atmosphere, in the present calculations a single ion-ion recombination coefficient of 2×10^{-6} cm^3/sec has been adopted for all pairs of ions at all pressures and temperatures.

3.4 OZONE CHEMISTRY.

The principal neutral reactions controlling the ozone concentration are the production mechanism:

$$O + O_2 + O_2 \rightarrow O_3 + O_2, \qquad (13)$$

and the destruction mechanism:

$$O + O_3 \rightarrow O_2 + O_2. \qquad (14)$$

Such reactions can occur for both ground and excited-state oxygen atoms, with different rate coefficients. In the radiolysis experiments of interest, excited oxygen atoms are so rapidly quenched by oxygen molecules that only the ground-state reactions need to be considered.

Ozone can also be destroyed by ion-molecule reactions, such as

$$O_2^- + O_3 \rightarrow O_3^- + O_2, \qquad (6)$$

$$O_3^- + O_3 \rightarrow O_2^- + 2O_2. \qquad (15)$$

This reaction sequence is "catalytic" in that the second reaction regenerates the O_2^- lost in the first reaction. A similar pair of destruction reactions could involve O_4^+ and O_5^+ in place of O_2^- and O_3^-, respectively.

The excited molecular oxygen states $O_2(^1\Delta)$ and $O_2(^1\Sigma)$ can dissociate ozone:

$$O_2(^1\Delta) + O_3 \rightarrow O + 2\ O_2, \qquad (16)$$

$$O_2(^1\Sigma) + O_3 \rightarrow O + 2\ O_2. \qquad (17)$$

However, at the pressures typical of radiolysis experiments, almost all of the oxygen atoms thus produced quickly react to re-form ozone. Hence, the role of these excited states is minor.

An upper limit to the amount of ozone that can be produced by radiolysis may be derived by neglecting all ozone destruction processes. With this neglect, every oxygen atom that is created yields one ozone molecule. From table 1, for each 100 eV of energy deposited in O_2, 7.0 oxygen atoms are produced, and also 1.0 O^+ ions, which rapidly charge exchange with O_2 to yield another oxygen atom. Hence, from these processes alone, $G(O_3) = 8.0$, where the G value is defined as the number of particles produced per 100 eV deposited. In addition, as discussed in section 3.2, each positive ion

created will, when it recombines with an electron or negative ion, produce two oxygen atoms, provided that other reactions have not converted the ions to more stable species like O_3^-. Since G (positive ions) = 3.25 (table 1), ion recombination can increase $G(O_3)$ by up to 6.5, giving a total upper limit of $G(O_3) = 8.0 + 6.5 = 14.5$.

3.5 CHEMISTRY COMPUTATION METHOD.

In the present study, time-dependent chemistry calculations have been made for situations corresponding to published oxygen radiolysis experiments. These calculations used the CHEM computer code developed at RDA, which employs a Gear integrator (Ref. 51) to solve numerically the coupled differential equations for the chemical kinetics. The calculations employed the initial production rates listed in table 1 and the rate coefficients listed in table 2. The results will be discussed in the next section.

SECTION 4

COMPUTED RESULTS AND COMPARISON WITH EXPERIMENT

4.1 OZONE PRODUCTION IN PULSE RADIOLYSIS.

Several studies have been carried out in which intense short-duration pulses of electrons were used to irradiate oxygen (Refs. 1, 52-54). The electron pulse generators used had peak electron energies of 600 keV to 2 MeV and pulse half-widths of around 30 nsec.

Typical species concentrations calculated for the pulse radiolysis of oxygen at 1 atmosphere are shown in Figure 1. The principal ions are O_4^+, O_2^- and O_4^-. The concentrations of electrons and O_2^+ are lower due to efficient attachment and clustering reactions. The ionic charge builds up during the period of electron irradiation, reaches a maximum, and then decays by ion-ion recombination, approximately as t^{-1} after the end of the pulse. At late times, as ozone appears, the ions O_3^- and O_5^+ become appreciable; however, by this time most of the ionization has dissipated.

Atomic oxygen, which is produced directly by electron bombardment, accumulates throughout the irradiation period. The deionization processes contribute additional atomic oxygen, so O continues to build up early in the deionization phase. At later times substantial ozone concentrations are produced from the association of O with O_2. Most of the ionization has disappeared by this time. The molecular oxygen metastable states $^1\Delta$ and $^1\Sigma$ decay over still longer time scales, and their dissociating reactions with O_3 tend to maintain a

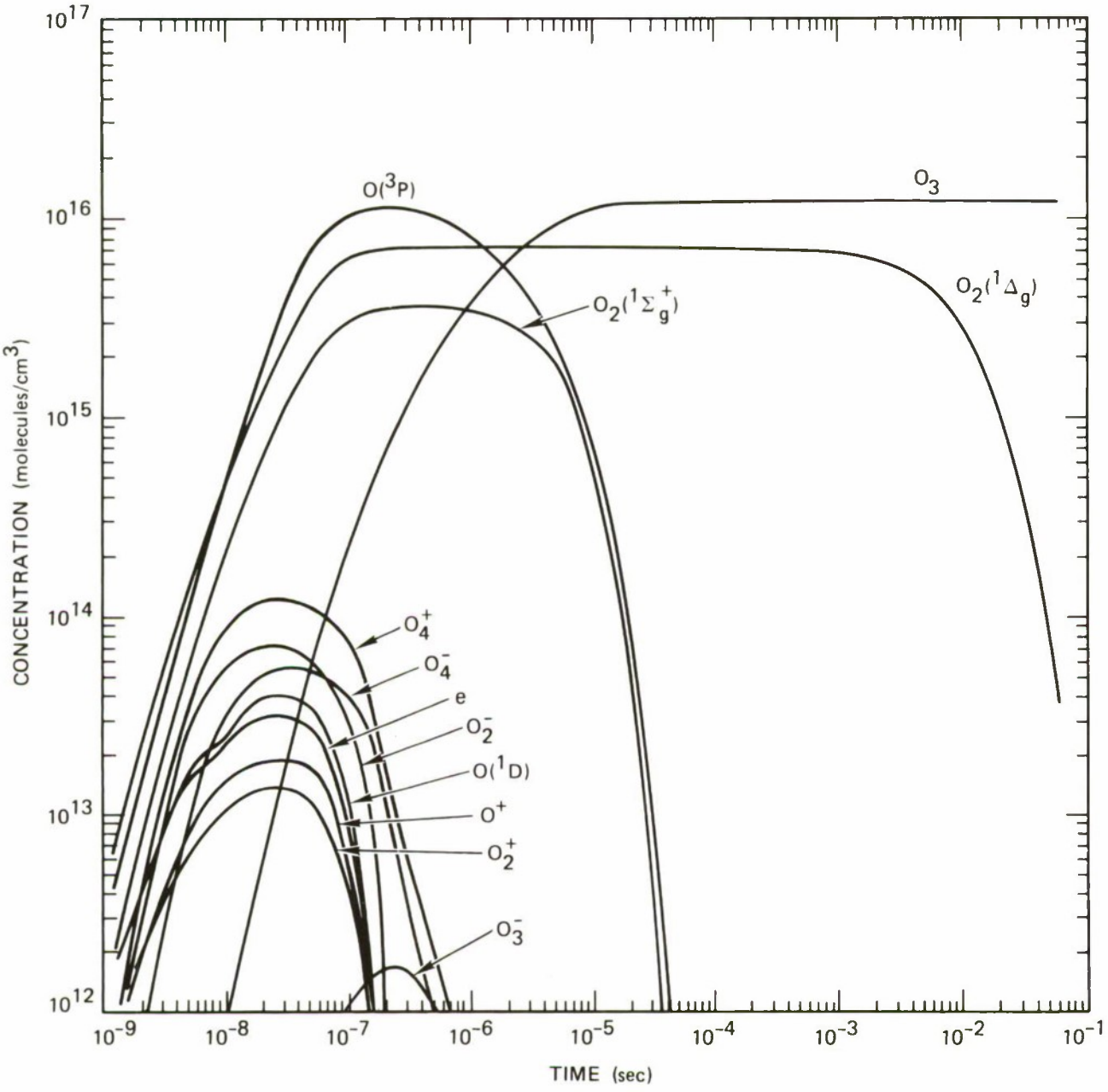

Figure 1. Time-dependent species concentrations in oxygen subject to a brief irradiation pulse varying with time as $t \exp(-t/t_o)$, where t_o = 22 nsec. The integrated dose is 1 x 10^6 rads, pressure 760 torr, and temperature 293 K.

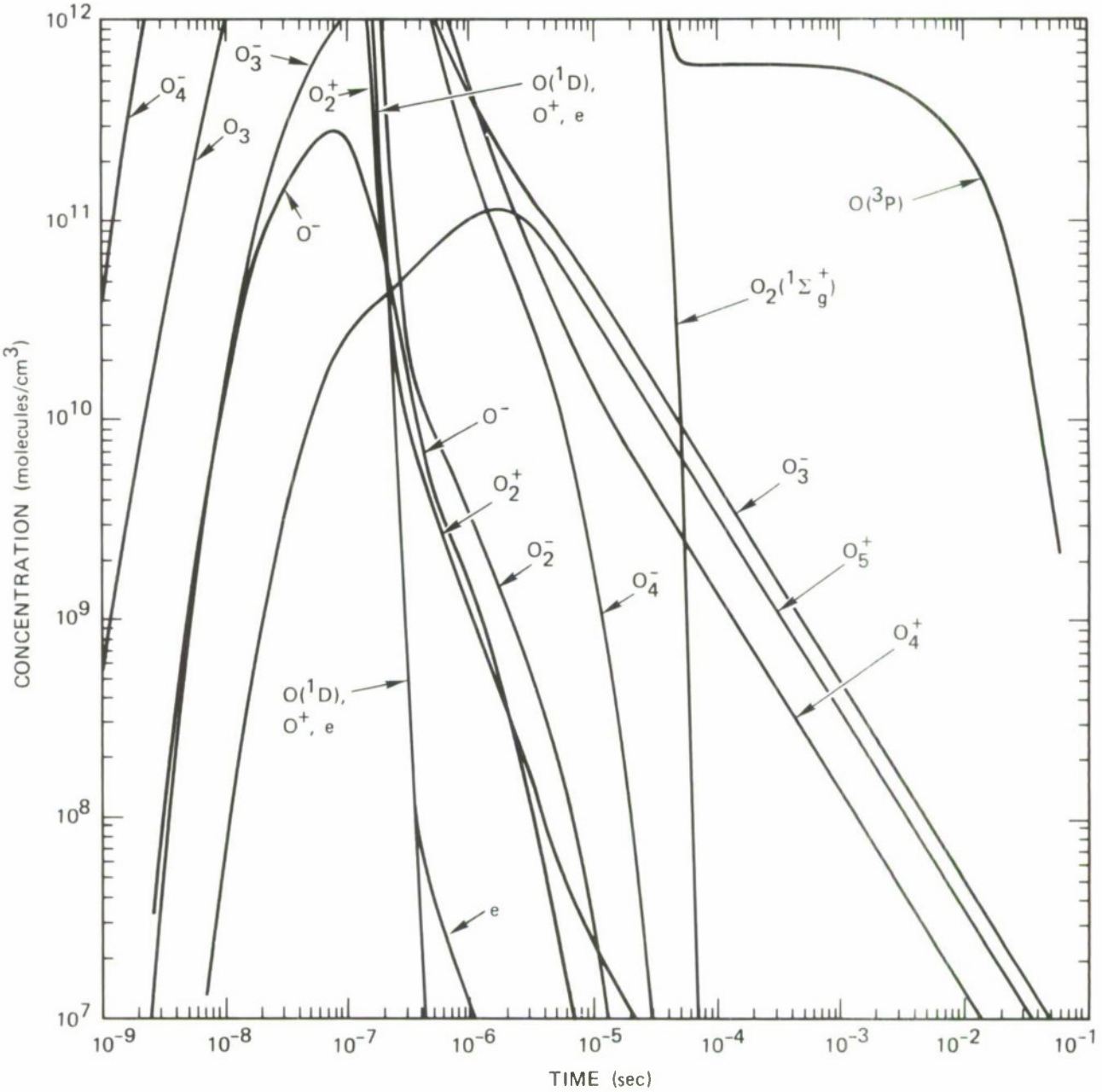

Figure 1. Time-dependent species concentrations in oxygen subject to a brief irradiation pulse varying with time as t exp(-t/t_o), where t_o = 22 nsec. The integrated dose is 1 x 10^6 rads, pressure 760 torr, and temperature 293 K. concluded).

low-level concentration of atomic oxygen, but this has little effect on the O_3 concentration or yield.

In table 3, predicted ozone G values from pulse radiolysis are compared with measured values. The agreement is reasonably good, considering the uncertainties in the computations and the measurements. The principal source of uncertainty in the calculations is probably the initial yields of various species in oxygen under electron bombardment. All of the pulse radiolysis experiments, and the corresponding calculations, show a high ozone yield, near the theoretical limit. Since figure 1 shows that at atmospheric pressure most of the charged-particle recombination occurs between O_4^+, O_4^- and O_2^-, this high ozone yield implies that recombination of these ions yields two oxygen atoms, as assumed in Table 2. Although these reactions are not listed in the DNA Reaction Rate Handbook (Ref. 33), the similar reaction, $O_2^+ + O_2^- \rightarrow O_2 + O_2$, is included. The present results strongly suggest that the products should be revised to $O_2 + 2\ O$.

Similar chemistry calculations were made for pulse radiolysis at 0.1 atm. The results show that O_2^+, O_4^+ and e are the major charged species in this case. The high ozone yield observed at this pressure by Willis et al. (Ref. 1) then indicates that $e + O_4^+$ yields two oxygen atoms. This result has been generally assumed (Ref. 33) but not previously confirmed.

4.2 EFFECT OF ELECTRON SCAVENGERS ON OZONE YIELD IN PULSE RADIOLYSIS.

An electron scavenger like sulfur hexafluoride (SF_6) can attach electrons to form SF_6^-, a negative ion that is more stable than O_2^- or O_4^-, and hence may not produce oxygen atoms

Table 3. Ozone yield in the pulse radiolysis of oxygen.
High dose rates: 10^{11} - 10^{13} rad/s (1 rad = 100 erg/g).
Gas temperature: 293 - 298 K.

Type of determination	O_2 pressure (torr)	$G(O_3)$ molec/100 eV)	Reference
Measurement	560	13.0*	52
Measurement	760	13.8±0.7	54
Measurement	30 - 800	12.8±0.6	1
Calculation	83, 830	14.0±0.9	1
Calculation	76, 760	13.8-14.4	This work
Theoretical limit	--	14.5	This work

*G value corrected for dosimetry in Ref. 1.

when it recombines with O_2^+ or O_4^+. These and other relevant reactions of SF_6 are summarized in table 4. Using these reactions and rate constants, chemistry calculations were made for the pulse radiolysis of oxygen containing 1 percent (by volume) of SF_6, corresponding to three published experiments (Refs. 1, 52, 53).

Table 5 compares the measured and calculated ozone yields. The calculated $G(O_3)$ = 8.0-8.1 (varying slightly with pressure) lies near the center of the range of measured values, $G(O_3)$ = 6.3-9.0. Since the calculations indicate that the major recombining ions are SF_6^-, O_4^+ and O_2^+, the reasonable agreement of the calculated with the measured ozone yields confirms the assumption (table 4) that recombination of these ions does not yield oxygen atoms.

4.3 OZONE BUILDUP DURING CONTINUOUS RADIOLYSIS.

A number of researchers have studied the effects of continuous radiolysis of pure oxygen (Refs. 1, 44, 55, 56). Most of these studies used gamma ray sources and irradiation intensities up to about 10^7 rad/hr, with total doses exceeding 10^8 rads in some cases. The difference between the energy sources employed in the pulse and steady radiolysis experiments (electrons versus gamma rays) has no direct bearing on the ion chemistry or ozone yield; the primary ionization products per unit energy absorbed are essentially the same in both cases. However, the steady radiolysis experiments involved much longer irradiation times and therefore significant ozone accumulation during the period of irradiation. Consequently, ions like O_3^- and O_5^+ are expected to be more important here than in the pulse radiolysis experiments.

Table 4. SF_6 chemistry.

Reaction	Rate Coefficient[a]	Reference or Footnote
$e + SF_6 \rightarrow SF_6^-$	2.2×10^{-7}	57, 58
$SF_6 + O_2^- \rightarrow SF_6^- + O_2$	7.0×10^{-11}	34
$SF_6 + O_4^- \rightarrow SF_6^- + 2\ O_2$	7.0×10^{-11}	b
$SF_6^- + O \rightarrow O^- + SF_6$	5.0×10^{-11}	34
$SF_6^- + O_3 \rightarrow O_3^- + SF_6$	3.2×10^{-11}	34
$SF_6^- + O^+ \rightarrow SF_6 + O$	2.0×10^{-6}	b
$SF_6^- + O_2^+ \rightarrow SF_6 + O_2$	2.0×10^{-6}	b
$SF_6^- + O_4^+ \rightarrow SF_6 + 2\ O_2$	2.0×10^{-6}	b
$SF_6^- + O_5^+ \rightarrow SF_6 + O_2 + O_3$	2.0×10^{-6}	b

Footnotes:

a. All rate coefficients have units of cm^3/sec.

b. Assumed by analogy.

Table 5. Ozone yield in pulse radiolysis of oxygen containing 1 percent (by volume) of sulfur hexafluoride; temperatures near 295 K.

Type of determination	Pressure (torr)	$G(O_3)$	References
Measurement	560	9.1*	52
Measurement	200-2000	7.9†	53
Measurement	400, 700	6.3±0.6	1
Calculation	76, 760	8.0,8.1	This work
Theoretical limit, without ionic contrib.	--	8.0	This work

*G value corrected for dosimetry as in Ref. 1.

†Normalized using $G(O_3)$ = 12.8 in pure oxygen at 760 torr (see table 3).

The present calculations for continuous radiolysis situations bear out this expectation. Although, during the very earliest period of the irradiation (corresponding to integrated doses of less than 10^3 rads) the ozone concentration is so small that little O_3^- or O_5^+ is predicted to form, by the time the ozone accumulates to levels that are easily measureable (around 10^4 rads) O_3^- becomes the dominant negative ion, and O_4^+ and O_5^+ the dominant positive ions. Consequently, the reasonable agreement of the calculated and measured ozone yields shown in table 6 supports the assumption (table 2) that recombination of O_3^- with O_4^+ or O_5^+ does not lead to dissociation. (The discrepancy of about 25 percent between the calculations and the measurements is not readily explainable but probably has little practical significance.)

As the oxygen irradiation time is lengthened and the total dose increases above about 10^5 rads, the calculated ozone production rate slows, due primarily to the assumed process, $O_3^- + O_3 \rightarrow O_2^- + 2\ O_2$ (Ref. 43), which effectively destroys two ozone molecules per reaction. (The well-known ozone destruction reaction, $O + O_3 \rightarrow 2\ O_2$, is much slower under most radiolysis conditions.) A qualitatively similar behavior has been observed in two sets of high-dose radiolysis measurements (Ref. 44, 56). However, Kircher et al. (Ref. 44) used "commercial" oxygen containing impurities that may have affected the ozone chemistry; moreover, their pressures were much higher than atmospheric. Consequently, no comparisons of Kircher's measurements with chemical calculations have been attempted.

Sears and Sutherland (Ref. 56) carried out experiments near atmospheric pressure using both all-glass vessels and quartz vessels having stopcocks lubricated with fluorocarbon grease.

Table 6. "Initial" ozone yield in the steady radiolysis of oxygen. ("Initial" implies low total dose, ~10^4 rads.) Gas temperatures are near 295 K unless otherwise indicated.

Type of determination	O_2 pressure	$G(O_3)$	References
Measurement	$(2-10)\times10^4$	5.9*	44
Measurement (200 K)	760	6.7*†	55
Measurement	665	6†‡	56
Measurement (77 K)	not stated	6.2±0.6	1
Theoretical estimate	--	7.5±0.9	1
Calculation	665	8 - 9	This work
Theoretical limit, without ionic contrib.	--	8.0	This work

*G value corrected for ozone-iodide stoichiometry in Ref. 1.

†G value corrected for dosimetry in Ref. 1.

‡See Ref. 1.

They observed that the ozone yields were greater in the vessels with stopcocks. This observation is consistent with the fact that many fluorine compounds will remove the negative charge from ions like O_3^-, and hence interfere with the $O_3^- + O_3$ destruction mechanism.

Unfortunately, Sears and Sutherland reported dose-dependent measurements only for the vessels with greased stopcocks. Their results are plotted in figure 2, along with calculations for pure oxygen and oxygen contaminated with 0.0044 percent (44 ppmv) of a hypothetical electron scavenger. The scavenger is assumed to have the same reactions as SF_6 (table 4), except that the charge transfer reactions with O^- and O_3^- proceed in the opposite direction (i.e., the scavenger has a greater electron affinity than O and O_3). The experimental points in figure 2 fall between the calculated points for pure and contaminated oxygen, strongly suggesting that the stopcock grease is producing an electron scavenger that removes the charge from O_3^-.

4.4 STEADY-STATE OZONE CONCENTRATIONS IN CONTINUOUS RADIOLYSIS.

With long enough irradiation times (corresponding to doses above approximately 10^7 rads) the chemical processes reach a steady state where ozone is destroyed as fast as it is formed. The ozone concentration thus eventually approaches a constant value. Sears and Sutherland (Ref. 56) present measurements for this concentration in all-glass (uncontaminated) vessels, as a function of the dose rate. These values are compared in figure 3 with values calculated using the reaction rates in table 2. The agreement is fairly good. The experimental values vary approximately--and the calculated values almost exactly--with the square root of

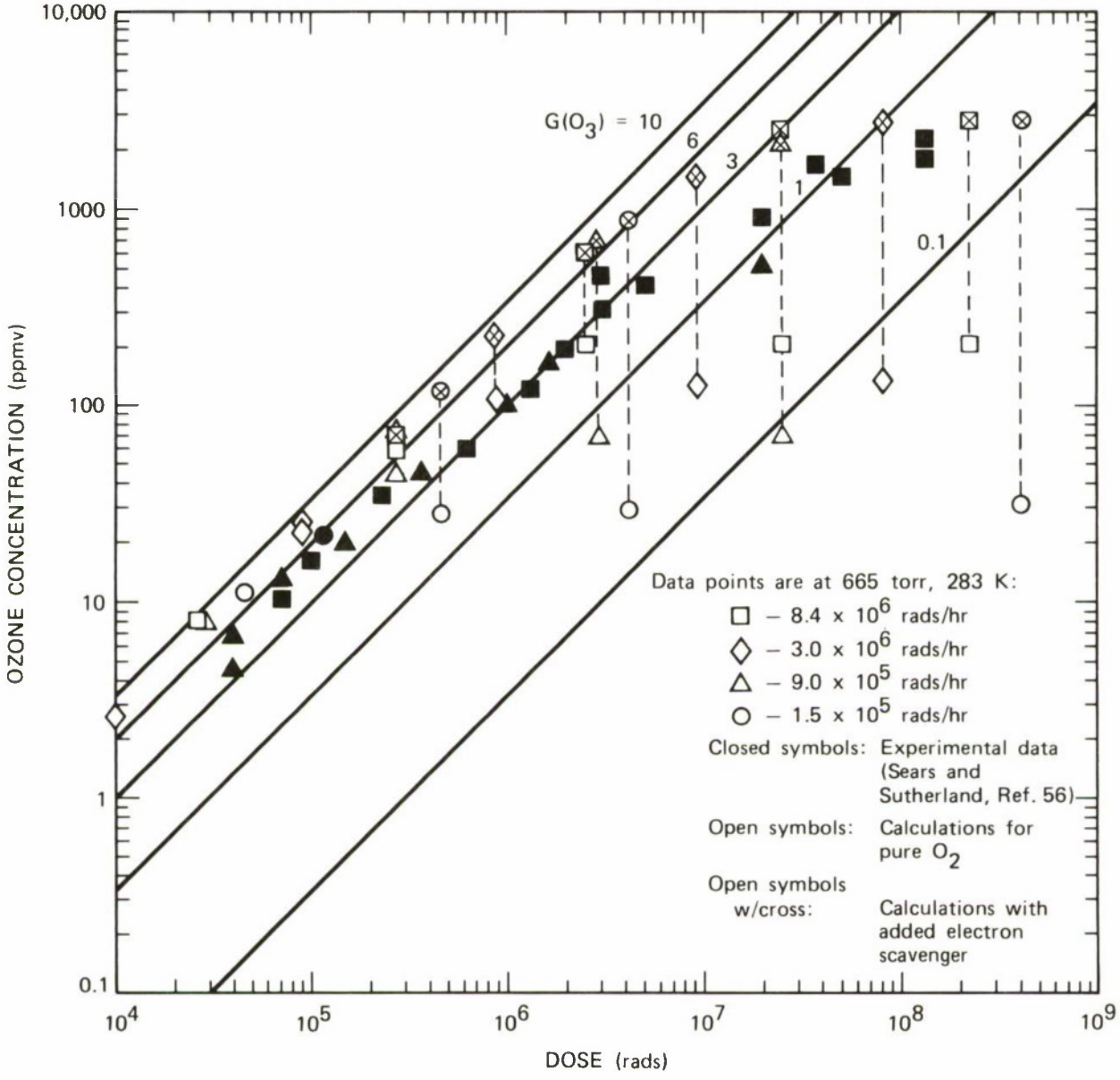

Figure 2. Measured and calculated ozone concentrations versus cumulative radiation dose for the continuous (slow) radiolysis of oxygen at 665 torr and 283 K. The diagonal lines correspond to loci of constant G values. For the calculated points connected by vertical dashed lines, the lower values correspond to pure oxygen while the upper values correspond to oxygen contaminated with 44 ppmv of a hypothetical electron scavenger (see text).

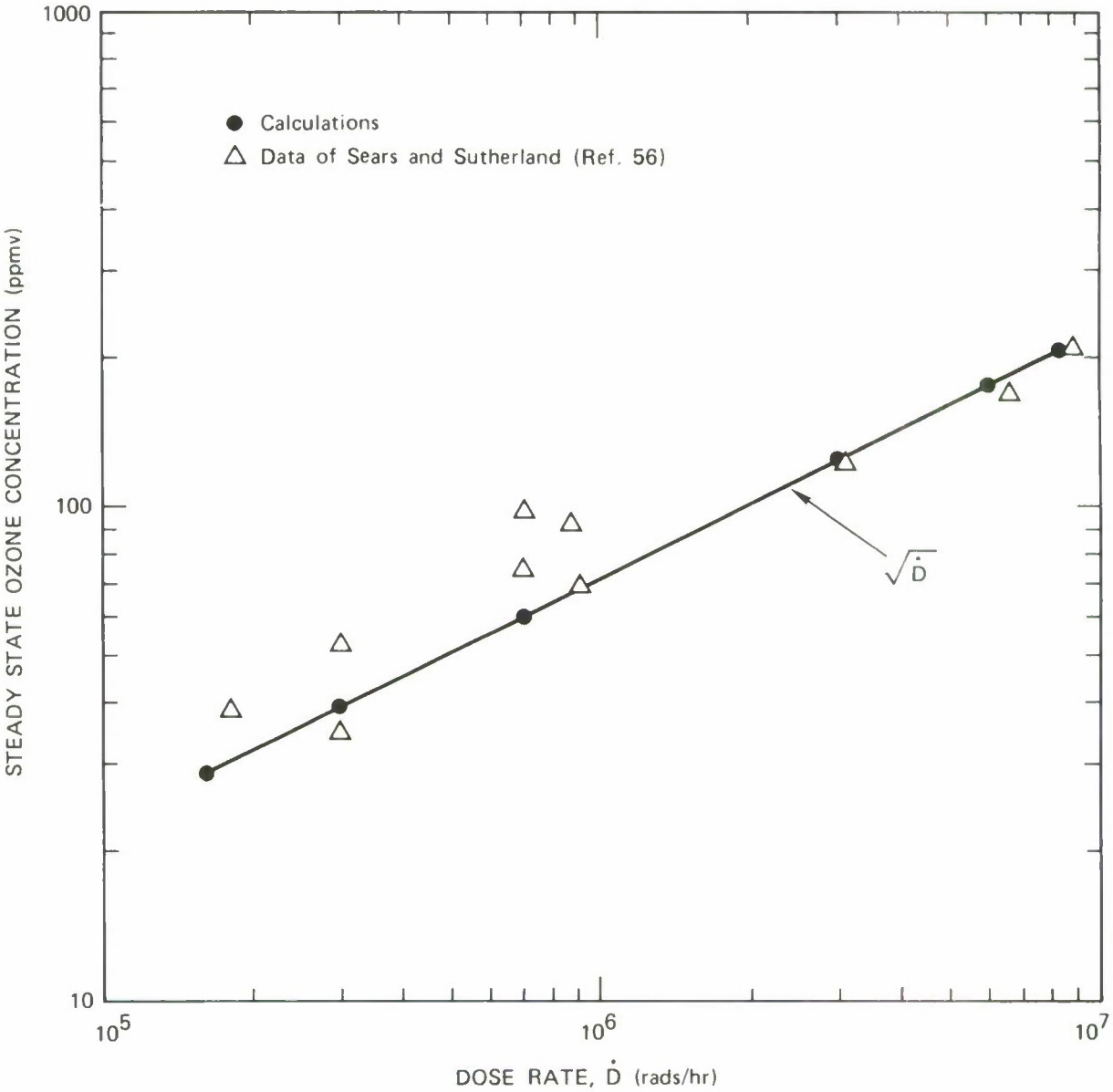

Figure 3. Comparison of measured and calculated steady-state ozone concentrations in irradiated oxygen as a function of dose rate.

the dose rate (solid line on figure 3). As pointed out by Sears and Sutherland, this behavior expected when the primary removal process is the reaction of a major ion with O_3, since in a steady state dominated by ion-ion recombination the ion concentration (of either sign) is proportional to the square root of the dose rate.

The agreement of the steady-state measurements with the calculations tends to support the assumed rate coefficient and products of the reaction $O_3^- + O_3 \rightarrow O_2^- + 2\ O_2$ (table 2). However, before this support can be considered strong, alternative destruction reactions must be ruled out. Note first, that to fit the radiolysis observations, the species reacting with and destroying ozone must be an odd oxygen species, like O_3^-, O_5^+ or $O(^1D)$; excited O_2 molecules can only break up ozone to give $O + O_2$, where the O atoms immediately re-form ozone. The decrease in ozone destruction in the presence of fluorocarbon grease (figure 2) strongly suggests a negative ion, since many fluorine compounds have large electron affinities and can scavenge charge from other negative ions. Moreover, if a neutral species (other than ozone) were the reactant, its primary removal process would have to be reaction with itself or with another free radical or ion, in order to yield the observed square root behavior. Enough is known about the potentially significant neutral species (in fact, they have been included in table 2 and in the calculations) to show that none satisfy this requirement.

Possible ozone destruction by ions like O^-, O_3^+ and O_5^+ should also be considered. However, the calculations show that the concentration of O^- in the radiolysis experiments is always much too small to contribute significantly to the ozone loss. The O_3^+ concentration is also small, because it is formed only

from O^+, which has a small concentration, and it is rapidly destroyed by charge transfer to O_2. (For these reasons, O_3^+ was not included in the present chemical calculations.)

On the other hand, the concentration of O_5^+ is large enough for it to destroy significant amounts of ozone, if the rate coefficient were large enough. At the lowest and highest dose rates employed by Sears and Sutherland, O_5^+ makes up about 20 and 60 percent, respectively, of the total positive ions, the remainder being O_4^+, which cannot destroy ozone. Hence, if the $O_5^+ + O_3$ and $O_3^- + O_3$ coefficients were equal, and both were a factor 1/1.6 smaller than the value used for the latter reaction in the calculations shown in figure 3, the low end of the curve would be raised about a factor of 1.6/1.2, while the high end would remain unchanged (neglecting the fairly small effect of the changed ozone amount on the O_5^+/O_4^+ ratio). This modified prediction would still fit the measurements reasonably well. However, if the O_5^+ rate coefficient were twice the O_3^- coefficient, there would be a significant discrepancy.

It follows that the $O_5^+ + O_3$ rate coefficient is probably less than 6×10^{-13} cm^3/s and may be much smaller. In addition, the value used for the O_3^- reaction in the calculations 1×10^{-12} cm^3/s, is probably an upper limit, since it would have to be lowered if O_5^+ contributes significantly to the destruction, or if the ion-ion recombination coefficient is smaller than the value of 2×10^{-6} cm^3/s used in the calculations (compare Ref. 50), since this would increase the O_3^- concentration. Accordingly, a reasonable choice for the room-temperature rate coefficient of the $O_3^- + O_3$ reaction is 5×10^{-13} cm^3/s, which may be correct to within a factor of 2. It probably varies with temperature roughly as exp(-1000/T), as deduced by Kircher et al. (Ref. 44)

for the temperature dependence of ozone destruction in high-pressure oxygen radiolysis. However, since the temperature may also shift the relative ion concentrations and change the ion-ion recombination coefficient, the observed temperature dependence may not be attributable solely to the $O_3^- + O_3$ reaction.

SECTION 5

CONCLUSIONS

The detailed electron-impact and chemical calculations carried out in this study have given results which agree within 25 percent with published measurements of ozone production in a variety of radiolysis experiments. The calculations employed electron-impact cross sections newly deduced from published data, and standard sets of reaction rate coefficients, with the addition of the following ion-ion recombination reactions:

$$O_4^+ + O_2^- \rightarrow 2\ O + 2\ O_2, \qquad (18)$$

$$O_4^+ + O_4^- \rightarrow 2\ O + 3\ O_2, \qquad (19)$$

$$O_4^+ + O_3^- \rightarrow 2\ O_2 + O_3, \qquad (20)$$

$$O_5^+ + O_3^- \rightarrow O_2 + 2\ O_3. \qquad (21)$$

(Some other recombination reactions were also added for completeness, but they have a negligible effect on the results.)

In conventional ion recombination experiments it has not been possible to identify the products of these reactions. The present analysis of the radiolysis experiments permits confident assignment of these products (except that in the last two reactions the O_3 might be replaced by $O + O_2$). Moreover, the products of the first reaction strongly imply that the $O_2^+ + O_2^-$ recombination reaction similarly yields

$2\ O + O_2$, instead of $2\ O_2$ as conventionally assumed. In addition, the analysis of the steady-state ozone concentration attained by prolonged irradiation, as a function of the dose rate, suggests that the ozone-destroying reaction

$$O_3^- + O_3 \rightarrow O_2^- + 2\ O_2 \qquad (15)$$

occurs with a rate coefficient within a factor of two of 5×10^{-13} cm^3/s at room temperature, and probably with a temperature variation of about exp (-1000/T). The reaction,

$$O_5^+ + O_3 \rightarrow O_4^+ + 2\ O_2 \qquad (22)$$

may also provide a significant ozone sink. However, it cannot be the dominant loss mechanism, so its rate constant cannot be larger than about 6×10^{-13} cm^3/s.

Calculations for oxygen containing traces of electron scavengers (such as fluorine compounds) show, in agreement with experiment, that these scavengers can affect the ozone yield in two opposing ways: In pulse radiolysis they can reduce the ozone yield by changing the ions to species that produce less atomic oxygen when they recombine. In continuous irradiation, where the ozone builds up and itself reduces the ozone yield by electron scavenging, addition of a stronger scavenger can remove the charge from O_3^-, thus inhibiting the $O_3^- + O_3$ reaction that destroys ozone, and increasing the ozone yield.

SECTION 6

LIST OF REFERENCES

1. C. Willis, A. W. Boyd, M. J. Young and D. A. Armstrong, "Radiation Chemistry of Gaseous Oxygen: Experimental and Calculated Yields," Canad. J. Chem. Vol. 48, 1970, pp. 1505-1514.

2. A.E.S. Green, C. H. Jackman and R. H. Garvey, "Electron Impact on Atmospheric Gases. 2. Yield Spectra," J. Geophys. Res., Vol. 82, 1977, pp. 5104-5111.

3. S. P. Khare, and A. Kumar, Jr., "Mean Energy Expended per Ion Pair by Electrons in Molecular Oxygen," J. Phys. B: Atom. Molec. Phys., Vol. 11, 1978, pp. 2403-2410.

4. A. Dalgarno and G. Lejeune, "The Absorption of Electrons in Atomic Oxygen," Planet. Space Sci., Vol. 19, 1971, pp. 1653-1667.

5. T. L. Stephens and A. L. Klein, Electron Energy Deposition in the Atmosphere, General Electric - TEMPO, GE75TMP-7 May 1975.

6. H. S. Porter, C. H. Jackman and A. E. S. Green, "Efficiencies for Production of Atomic Nitrogen and Oxygen by Relativistic Proton Impact in Air," J. Chem. Phys., Vol. 65, 1976, pp. 154-167.

7. C. H. Jackman, R. H. Garvey and A. E. S. Green, "Electron Impact on Atmospheric Gases. I. Updated Cross Sections," J. Geophys. Res., Vol. 82, 1977, pp. 5081-5090.

8. F. Linder and H. Schmidt, "Experimental Study of Low Energy e-O_2 Collision Processes," Z. Naturforsch., Vol. 26a, 1971, pp. 1617-1625.

9. S. Trajmar, D. C. Cartwright and W. Williams, "Differential and Integral Cross Sections for the Electron Impact Excitation of the $a^1\Delta_g$ and $b^1\Sigma_g$ States of O_2," Phys. Rev. A, Vol. 4, 1971, pp. 1482-1492.

10. S. Trajmar, W. Williams and A. Kupperman, "Angular Dependence of Electron Impact Excitation Cross Sections of O_2," J. Chem. Phys., Vol. 56, 1972, pp. 3759-3765.

11. K. Wakiya, "Differential and Integral Cross Sections for the Electron Impact Excitation of O_2. II. Optically Forbidden Transitions from the Ground State," J. Phys. B: Atom. Molec. Phys., Vol. 11, 1978, pp. 3931-3938.

12. K. Wakiya, "Differential and Integral Cross Sections for the Electron Impact Excitation of O_2. I. Optically Allowed Transitions from the Ground State," J. Phys. B: Atom. Molec. Phys., Vol. 11, 1978, pp. 3913-3930

13. T. W. Shyn, private communication, Oct. 1985.

14. P. H. Krupenie, "The Spectrum of Molecular Oxygen," J. Phys. Chem. Ref. Data, Vol. 1, 1972, pp. 423-534.

15. F. M. Matsunaga and K. Watanabe, "Total and Photoionization Coefficients and Dissociation Continua of O_2 in the 580 - 1070 Å Region," Sci. Light, Vol. 16, 1967, pp. 31-42.

16. D. Rapp and P. Englander-Golden, "Total Cross Sections for Ionizatioin and Attachment in Gases by Electron Impact. I. Positive Ionization," J. Chem. Phys., Vol. 43, 1965, pp. 1464-1479.

17. B. L. Schram, F. J. De Heer, M. J. Van der Wiel and J. Kistemaker, "Ionization Cross Sections for Electrons (0.6-20 keV) in Noble and Diatomic Gases," Physica, Vol. 31, 1965, pp. 94-112.

18. B. L. Schram, H. R. Moustafa, J. Schutten and F. J. De Heer, "Ionization Cross Sections for Electrons (100-600 eV) in Noble and Diatomic Gases," Physica, Vol. 32, 1966, pp. 734-740.

19. B. R. Turner, J. A. Rutherford and D.M.J. Compton, "Abundance of Excited Ions in O^+ and O_2^+ Ion Beams," J. Chem. Phys., Vol. 48, 1968, pp. 1602-1608.

20. D. Rapp, P. Englander-Golden and D. D. Briglia, "Cross Sections for Dissociative Ionization of Molecules by Electron Impact," J. Chem. Phys., Vol. 42, 1965, pp. 4081-4085.

21. V. I. Korol', S. M. Kishko and V. V. Skubenich, "Determination of Excitation Cross Sections of Some O_2^+ Bands by the Method of Intersecting Beams," Ukrain. Phys. J., Vol. 13, 1969, pp. 875-876.

22. J. W. McConkey and J. M. Woolsey, "Excitation of O_2^+ Bands of Electron Impact," J. Phys. B, Vol. 2, 1969, pp. 529-533.

23. P. Erman and M. Larson, "Lifetimes of Excited Levels in some Important Ion-Molecules," Phys. Scripta, Vol. 15, 1977, pp. 335-338.

24. J.F.M. Aorts and F. J. De Heer, private communication to J. W. McConkey, 1968 (see Ref. 22).

25. V. T. Koppe, et al., "Effective Cross Sections and Excitation Functions of the Bands of the First Negative System of O_2^+ and Some O I and O II Multiplets," Opt. Spectry., Vol. 33, 1972, pp. 326-327.

26. W. L. Borst and E. C. Zipf, "Excitation of O_2^+ First Negative Bands by Electron Impact on O_2," Phys. Rev. A, Vol. 1, 1970, pp. 1410-1415.

27. B. N. Srivastava, "Emission Cross Section for the First Negative Band System of Oxygen Produced by Electron Impact," J. Quant. Spectr. Rad. Transfer, Vol. 10, 1970, pp. 1211-1217.

28. A.E.S. Green and S. K. Dutta, "Semi-Empirical Cross Sections for Electron Impacts," J. Geophys. Res., Vol. 72, 1967, pp. 3933-3941.

29. J.A.R. Samson, J. L. Gardner and G. N. Haddad, "Total and Partial Photoionizaton Cross-Sections of O_2 from 100 to 800 Å," J. El. Spectr. Rel. Phen., Vol. 12, 1977, pp. 281-292.

30. J. Glosik, A. B. Rakshit, N. D. Twiddy, N. G. Adams and D. Smith, "Measurement of the Rates of Reaction of the Ground and Metastable Excited States of O_2^+, NO^+ and O^+ with Atmospheric Gases at Thermal Energy," J. Phys. B., Vol. 11, 1978, pp. 3365-3379.

31. L. G. Christophorou, Atomic and Molecular Radiation Physics, Wiley-Interscience, New York, 1971, p. 36.

32. G. G. Meisels, "Gas-Phase Dosimetry by Use of Ionization Measurements," J. Chem. Phys., Vol. 41, 1964, pp. 51-56.

33. Defense Nuclear Agency Reaction Rate Handbook, DNA 1948H, M. Bortner and T. Baurer, Eds., G. E. Tempo, Santa Barbara, Revision 8, 1979.

34. D. L. Albritton, "Ion-neutral Reaction Rate Constants Measured in Flow Reactors through 1977," Atom. Data Nuc. Tables, Vol. 22, 1978, pp. 1-101.

35. D. L. Baulch, et al., "Evaluated Kinetic and Photochemical Data for Atmospheric Chemistry," J. Phys. Chem. Ref. Data, Vol. 9, 1980, pp. 295-471.

36. W. B. DeMore, et al., "Chemical Kinetics and Photochemical Data for Use in Stratospheric Modeling: Evaluation Number 7," Jet Propulsion Laboratory Publ. 85-37, 1985.

37. D. L. Baulch, et al., "Evaluated Kinetic and Photochemical Data for Atmospheric Chemistry: Supplement I. CODATA Task Group on Chemical Kinetics," J. Phys. Chem. Ref. Data, Vol. 11, 1982, pp. 327-496.

38. R. F. Hampson, "Chemical Kinetic and Phtochemical Data Sheets for Atmospheric Reactions," U. S. Dept. of Transportation Report FAA-EE-80-17, Washington, D.C., 1980.

39. H. Bohringer and F. Arnold, "Temperature Dependence of Three-body Association Reactions from 45 to 400 K. The Reactions $N_2^+ + 2N_2 \rightarrow N_4^+ + N_2$ and $O_2^+ + 2O_2 \rightarrow O_4^+ + O_2$," J. Chem. Phys., Vol. 77, 1982, pp. 5534-5541.

40. J. D. Payzant, A. J. Cunningham and P. Kebarle, "Temperature Dependence of the Rate Constants for the Third Order Reactions: $O_2^+ + 2O_2 = O_4^+ + O_2$ and $O_4^+ + 2O_2 = O_6^+ + O_2$," J. Chem. Phys., Vol. 59, 9173, pp. 5615-5619.

41. D. C. Conway and G. S. Janik, "Determination of the Bond Energies for the Series $O_2^+-O_2$ through $O_2^+-O_{10}$," J. Chem. Phys., Vol. 53, 1970, pp. 1859-1866.

42. I. Dotan, J. A. Davidson, F. C. Fehsenfeld and D. L. Albritton, "Reactions of $O_2^+ \cdot O_2$ with CO_2, O_3, and CH_4 and $O_2^+ \cdot O_3$ with H_2O and CH_4 and Their Role in Stratospheric Ion Chemistry," J. Geophys. Res., Vol. 83, 1978, pp. 4036-4038.

43. P. Harteck, S. Dondes and B. Thompson, "Ozone: Decomposition by Ionizing Radiation," Science, Vol. 147, 1965, pp. 393-394.

44. J. F. Kircher, J. S. McNulty, J. L. McFarling and A. Levy, "Irradiation of Gaseous and Liquid Oxygen," Radiation Res., Vol. 13, 1960, pp. 452-465.

45. L. B. Loeb, Basic Processes of Gaseous Electronics, U. California Press, Berkeley, 1961, Chapter VI, pp. 497-596.

46. D. R. Bates, "Recombination of Small Ions in the Troposphere and Lower Stratosphere," Planet. Space Sci., Vol. 30, 1982, pp. 1275-1282.

47. S. A. Lawton, S. E. Novick, H. P. Broida and A. V. Phelps, "Quenching of Optically Pumped $O_2(b^1S_g^+)$ by Ground State O_2 Molecules," J. Chem. Phys., Vol. 66, 1977, pp. 1381-1382.

48. K. Tachibana and A. V. Phelps, "Excitation of the $O_2(a^1D_g)$ State by Low Energy Electrons," J. Chem. Phys., Vol. 75, 1981, pp. 3315-3320.

49. T. G. Slanger and G. Black, "Interactions of $O_2(b^1S_g^+)$ with $O(^3P)$ and O_3," J. Chem. Phys., Vol. 70, 1979, pp. 3434-3438.

50. C. J. Wood, R. A. Back and D. H. Dawes, "Ion Lifetimes in Gaseous Radiolysis Systems," Canad. J. Chem., Vol. 45, 1967, pp. 3071-3078.

51. C. W. Gear, "The Numerical Integration of Ordinary Differential Equations," Math Comp., Vol. 21, 1967, pp. 146-156.

52. G. M. Meaburn, D. Perner, J. LeCalve and M. Bourene, "A Pulsed-radiolysis Study of Atomic Oxygen Reactions in the Gas Phase," J. Phys. Chem., Vol. 72, 1968, pp. 3920-3925.

53. G.R.A. Johnson, and D. D. Wilkey, "Pressure Dependence of the Yield of Ozone from the Pulse Radiolysis of Oxygen at High Dose Rates," Chem. Comm., 1969, pp. 1455-1456.

54. J. A. Ghormley, C. J. Hochanadel and J. W. Boyle, "Yield of Ozone in the Pulse Radiolysis of Gaseous Oxygen at Very High Dose Rate. Use of This System as a Dosimeter," J. Chem. Phys., Vol. 50, pp. 1969, 419-423.

55. Johnson, G.R.A. and J. M. Warman, "Formation of Ozone from Oxygen by the Action of Ionizing Radiations," Disc. Faraday Soc. Vol. 37, 1964, pp. 87-95.

56. Sears, J. T., and J. W. Sutherland, "Radiolytic Formation and Decomposition of Ozone," J. Phys. Chem., Vol. 72, 1968, pp. 1166-1171.

57. F. C. Fehsenfeld, "Electron Attachment to SF_6," J. Chem. Phys., Vol. 53, 1970, pp. 2000-2004.

58. J. M. Warman, K. M. Bansal and R. W. Fessenden, "On the Pressure Dependence of Electron Attachment to O_2," Chem. Phys. Lett., Vol. 12, 1971, pp. 211-213.

DISTRIBUTION LIST

DEPARTMENT OF DEFENSE

ASST TO THE SECY OF DEFENSE ATOMIC ENERGY
ATTN: EXECUTIVE ASSISTANT

BOSTON COLLEGE, THE TRUSTEES OF
2 CYS ATTN: CHAIRMAN DEPT OF CHEMISTRY
2 CYS ATTN: CHAIRMAN DEPT OF PHYSICS

DEFENSE INTELLIGENCE AGENCY
ATTN: RTS-2B

DEFENSE NUCLEAR AGENCY
ATTN: RAAE K SCHWARTZ
ATTN: RAAE P CROWLEY
ATTN: RAAE P LUNN
4 CYS ATTN: STTI-CA

DEFENSE TECHNICAL INFORMATION CENTER
12 CYS ATTN: DD

FIELD COMMAND DEFENSE NUCLEAR AGENCY
ATTN: FCTT
ATTN: FCTT W SUMMA

FIELD COMMAND DNA DET 2
LAWRENCE LIVERMORE NATIONAL LAB
ATTN: FC-1

JOINT STRAT TGT PLANNING STAFF
ATTN: JLKS

UNDER SECY OF DEF FOR RSCH & ENGRG
ATTN: DEFENSIVE SYSTEMS
ATTN: STRAT & SPACE SYS(OS)
ATTN: STRAT & THTR NUC FOR F VAJDA

DEPARTMENT OF THE ARMY

HARRY DIAMOND LABORATORIES
2 CYS ATTN: SCHLD-NW-P

U S ARMY ATMOSPHERIC SCIENCES LAB
3 CYS ATTN: SLCAS-AE-E

U S ARMY BALLISTIC RESEARCH LAB
ATTN: SLCBR-SS-T TECH LIB

U S ARMY FOREIGN SCIENCE & TECH CTR
ATTN: DRXST-SD

U S ARMY NUCLEAR & CHEMICAL AGENCY
ATTN: LIBRARY

U S ARMY RESEARCH OFFICE
ATTN: R MACE

U S ARMY STRATEGIC DEFENSE COMMAND
ATTN: ATC-O W DAVIES

USA ELECT WARFARE/SEC,SURV & TARGET ACQ CTR
ATTN: AMSEL-EW-SS S KRONENBERG

DEPARTMENT OF THE NAVY

NAVAL AIR PROPULSION CENTER
ATTN: PE34 F HUSTED

NAVAL POSTGRADUATE SCHOOL
ATTN: CODE 1424 LIBRARY

NAVAL RESEARCH LABORATORY
ATTN: CODE 2000 J BROWN
ATTN: CODE 2627 TECH LIB
ATTN: CODE 4128.2 J JOHNSON
ATTN: CODE 4139 D MCNUTT
ATTN: CODE 4700 W ALI
ATTN: CODE 4700 S OSSAKOW
ATTN: CODE 4720 J DAVIS
ATTN: CODE 4780 D STROBEL

NAVAL SURFACE WEAPONS CENTER
ATTN: CODE X211 TECH LIB

NAVAL WEAPONS SUPPORT CENTER
ATTN: CODE 6054 T ELLIS

SPACE & NAVAL WARFARE SYSTEMS CMD
ATTN: PD 50TD

DEPARTMENT OF THE AIR FORCE

AIR FORCE GEOPHYSICS LABORATORY
4 CYS ATTN: CA A STAIR
2 CYS ATTN: LID W SWIDER
2 CYS ATTN: LIU R HUFFMAN
2 CYS ATTN: LS R MURPHY
2 CYS ATTN: LSI R SHARMA
2 CYS ATTN: LSP D PAULSON
ATTN: LSP D SMITH
2 CYS ATTN: LSP R NADILE
2 CYS ATTN: LYD K CHAMPION

AIR FORCE OFFICE OF SCIENTIFIC RSCH
ATTN: AFOSR/NC
ATTN: ASOSR/NP MAJ JOHN PRINCE

DEPARTMENT OF THE AIR FORCE (CONTINUED)

AIR FORCE SYSTEMS COMMAND
ATTN: DLAE
ATTN: DLTW
ATTN: DLXP
ATTN: SDR

AIR FORCE TECHNICAL APPLICATIONS CTR
ATTN: TX

AIR FORCE WEAPONS LABORATORY, AFSC
ATTN: SUL

AIR UNIVERSITY LIBRARY
ATTN: AUL-LSE

DEPUTY CHIEF OF STAFF/AFRDS
3 CYS ATTN: AFRDS SPACE SYS & C3 DIR

ROME AIR DEVELOPMENT CENTER, AFSC
ATTN: OCD J SIMONS

SPACE DIVISION/AQ
ATTN: WE

SPACE DIVISION/YG
ATTN: YGD

SPACE DIVISION/YN
ATTN: YN

STRATEGIC AIR COMMAND/INCR
ATTN: INCR

STRATEGIC AIR COMMAND/NRI-STINFO
ATTN: NRI/STINFO

DEPARTMENT OF ENERGY

DEPARTMENT OF ENERGY
ATTN: OMA, DP-22

UNIVERSITY OF CALIFORNIA
LAWRENCE LIVERMORE NATIONAL LAB
ATTN: L-10 A GROSSMAN
ATTN: L-262 D WUEBBLES
ATTN: L-325 G HAUGAN
ATTN: L-48 E WOODWARD
ATTN: L-71 J CHANG
ATTN: L-84 H KRUGER

LOS ALAMOS NATIONAL LABORATORY
ATTN: D SAPPENFIELD
ATTN: G M SMITH
ATTN: M PONGRATZ
ATTN: M SANDFORD
ATTN: P364 REPORT LIBRARY
ATTN: R JEFFRIES
ATTN: REPORT LIBRARY
ATTN: T BIENIEWSKI

SANDIA NATIONAL LABORATORIES
ATTN: L ANDERSON 2000
ATTN: M KRAMM 5230
ATTN: ORG 314 W D BROWN
ATTN: TECH LIB 3141 RPTS RCVG CLRK

OTHER GOVERNMENT

CENTRAL INTELLIGENCE AGENCY
ATTN: OSWR/NED

DEPARTMENT OF COMMERCE
ATTN: SEC OFC FOR J DEVOE
ATTN: SEC OFC FOR M KRAUSS
ATTN: SEC OFC FOR R LEVINE
ATTN: SEC OFC FOR S ABRAMOWITZ

NASA
3 CYS ATTN: A AIKIN
ATTN: CODE 6801 A TEMPKIN

NASA
ATTN: N-245-3 R WHITTEN

NASA
ATTN: J GRAY

NASA HEADQUARTERS
ATTN: 1 SCHARDT

NATIONAL OCEANIC & ATMOSPHERIC ADMIN
3 CYS ATTN: E FERGUSON
3 CYS ATTN: F FEHSENFELD

U S DEPARTMENT OF COMMERCE
ATTN: W UTLAUT

DEPARTMENT OF DEFENSE CONTRACTORS

AERODYNE RESEARCH, INC
ATTN: C KOLB

AEROSPACE CORP
ATTN: I GARFUNKEL
ATTN: J REINHEIMER
ATTN: J STRAUS
ATTN: N COHEN

AVCO EVERETT RESEARCH LAB, INC
ATTN: C VON ROSENBERG JR

BERKELEY RSCH ASSOCIATES, INC
ATTN: J WORKMAN
ATTN: S BRECHT

BOSTON COLLEGE
ATTN: E HEGBLOM
ATTN: W GRIEDER

CALIFORNIA, UNIVERSITY AT RIVERSIDE
ATTN: J PITTS JR

DEPT OF DEFENSE CONTRACTORS (CONTINUED)

CALSPAN CORP
ATTN: C TREANOR
ATTN: J GRACE
ATTN: M DUNN

COMPUTER SCIENCES CORP
ATTN: F EISENBARTH

CONCORD SCIENCES CORP
ATTN: E SUTTON

CORNELL UNIVERSITY
ATTN: M KELLY

DENVER, UNIVERSITY OF
ATTN: SEC OFFICER FOR D MURCRAY

ENVIRONMENTAL RSCH INST OF MICHIGAN
ATTN: IRIA LIBRARY

EOS TECHNOLOGIES, INC
ATTN: B GABBARD

GENERAL ELECTRIC CO
ATTN: R EDSALL

GEO CENTERS, INC
ATTN: E MARRAM

HSS, INC
ATTN: M SHULER

INSTITUTE FOR DEFENSE ANALYSES
ATTN: E BAUER
ATTN: H WOLFHARD

KAMAN SCIENCES CORP
ATTN: E CONRAD

KAMAN TEMPO
ATTN: B GAMBILL
5 CYS ATTN: DASIAC
ATTN: R RUTHERFORD

KAMAN TEMPO
ATTN: DASIAC

LOCKHEED MISSILES & SPACE CO, INC
ATTN: B MCCORMAC
ATTN: J CLADIS
ATTN: J KUMER
ATTN: J PEREZ
ATTN: J REAGAN
ATTN: M WALT
ATTN: R SEARS

MISSION RESEARCH CORP
ATTN: D ARCHER
ATTN: D SOWLE
ATTN: F GUIGLIANO
ATTN: M SCHEIBE
ATTN: R HENDRICK
ATTN: R KILB
2 CYS ATTN: TECH LIBRARY

MISSION RESEARCH CORP
ATTN: C LONGMIRE
ATTN: R PETERKIN
ATTN: R STELLINGWERF

PACIFIC-SIERRA RESEARCH CORP
ATTN: H BRODE, CHAIRMAN SAGE

PHOTOMETRICS, INC
ATTN: I L KOFSKY

PHYSICAL RESEARCH, INC
ATTN: T STEPHENS

PHYSICAL RESEARCH, INC
ATTN: J DEVORE

PHYSICAL SCIENCE LAB
ATTN: W BERNING

PHYSICAL SCIENCES, INC
ATTN: G CALEDONIA

PITTSBURGH, UNIV OF THE COMMONWEALTH
ATTN: M BIONDI

PRINCETON UNIVERSITY
ATTN: LIBRARIAN

R & D ASSOCIATES
2 CYS ATTN: F GILMORE
ATTN: H ORY
2 CYS ATTN: R TURCO

R & D ASSOCIATES
ATTN: J ROSENGREN

RAND CORP
ATTN: C CRAIN
ATTN: P DAVIS

RAND CORP
ATTN: B BENNETT

SCIENCE APPLICATIONS INTL CORP
ATTN: D HAMLIN

SCIENCE APPLICATIONS INTL CORP
ATTN: R LEADABRAND

SCIENCE APPLICATIONS INTL CORP
ATTN: E HYMAN

DEPT OF DEFENSE CONTRACTORS (CONTINUED)

SPACE DATA CORP
ATTN: S FISHER

SRI INTERNATIONAL
ATTN: D MCDANIEL
ATTN: W CHESNUT

STEWART RADIANCE LABORATORY
ATTN: R HUPPI

TECHNOLOGY INTERNATIONAL CORP
ATTN: W BOQUIST

TELEDYNE BROWN ENGINEERING
ATTN: F LEOPARD
ATTN: MS-12 TECHNICAL LIBRARY
ATTN: N PASSINO

TOYON RESEARCH CORP
ATTN: J ISE

UTAH STATE UNIVERSITY
ATTN: A STEED
ATTN: C WYATT
ATTN: D BAKER
ATTN: K BAKER DIR ATMOS & SPACE SCI

VISIDYNE, INC
ATTN: J CARPENTER

WAYNE STATE UNIVERSITY
ATTN: R KUMMLER SCIENCE LIB

WAYNE STATE UNIVERSITY
ATTN: W KAUPPILA

DIRECTORY OF OTHER

GOVERNMENT PUBLICATIONS LIBRARY-M
ATTN: J WINKLER

YALE UNIVERSITY
ATTN: ENGINEERING DEPT